STRUCTURAL DAMAGE DETECTION BY FUZZY- GAUSSIAN TECHNIQUE

D. R. Parhi[1] and H. C. Das[2]

[1]*Department of Mechanical Engineering, N.I.T. Rourkela, Orissa, India, 769008,*
Email: dayalparhi@yahoo.com
[2]*Department of Mechanical Engineering, I.T.E.R, Bhubaneswar, Orissa, India, 751010,*

Received 11 December 2007; accepted 3 March 2008

ABSTRACT

The method of detecting crack location and its intensity in beam structures by fuzzy logic techniques has been considered in this paper. The fuzzy logic controller used here comprises of six input parameters and two output parameters. Gaussian member ship functions are used for the fuzzy controller. The input parameters to the fuzzy- Gaussian controller are relative deviation of first three natural frequencies and relative value of first three mode shapes percentage deviation. The output parameters of the fuzzy inference system are relative crack depth and relative crack location. At the beginning theoretical analyses have been outlined for cracked cantilever beam to calculate the vibration parameters such as natural frequencies and mode shapes. The local stiffnesses at the crack location are influenced by crack intensity and are calculated using strain energy release rate. A set of boundary conditions are considered involving the effect of crack location. A series of fuzzy rules are derived from vibration parameters which are finally used for prediction of crack location and its intensity. The proposed approach is verified by comparing with the results obtained from the developed experimental setup.

Key words: Vibration, crack, natural frequency, mode shape, fuzzy-gaussian controller.

NOMENCLATURE

a_1	= depth of crack
A	= cross-sectional area of the beam
A_i i = 1to 12	= unknown coefficients of matrix A
B	= width of the beam
B_1	= vector of exciting motion
C_u	$= (\frac{E}{\rho})^{1/2}$
C_y	$= (\frac{EI}{\mu})^{1/2}$
E	= young's modulus of elasticity of the beam material
fmd	= relative first mode difference
fnf	= relative first natural frequency
F_i i = 1, 2	= experimentally determined function

i, j = variables
J = strain-energy release rate
$K_{1,i}$ $i = 1, 2$ = stress intensity factors for P_i loads
$\overline{K}_u$ = $\omega L/C_u$
$\overline{K}_y$ = $\left(\frac{\omega L^2}{C_y}\right)^{1/2}$
K_{ij} = local flexibility matrix elements
L = length of the beam
L_1 = location (length) of the crack from fixed end
M_i $i=1,4$ = compliance constant
P_i $i=1,2$ = axial force ($i=1$), bending moment ($i=2$)
Q = stiffness matrix for free vibration.
Q_1 = stiffness matrix for forced vibration
rcd = relative crack depth
rcl = relative crack location
smd = relative second mode difference
snf = relative second natural frequency
tmd = relative third mode difference
tnf = relative third natural frequency
u_i $i=1,2$ = normal functions (longitudinal) $u_i(x)$
x = co-ordinate of the beam
y = co-ordinate of the beam
Y_0 = amplitude of the exciting vibration
y_i $i=1,2$ = normal functions (transverse) $y_i(x)$
W = depth of the beam
ω = natural circular frequency
β = relative crack location (L_1/L)
μ = $A\rho$
ρ = mass-density of the beam
ξ_1 = relative crack depth (a_1/W)
V = aggregate (union)
Λ = minimum (min) operation
$\forall$ = for every

1 INTRODUCTION

Structural systems undergo premature failure due to presence of crack. Therefore intensive research has been going on amongst the scientists and engineers to find an effective methodology to predict the location and intensity of damage beforehand. Different researchers have discussed damage detection of vibrating structures in various ways. They are summarized below.

The method of crack localization and sizing in a beam has been obtained from free and forced response measurements by Karthikeyan et al. (Karthikeyan et al 2007). This method has been illustrated through numerical examples. The prediction for the crack location and size are in agreement taking the noise and measurement error in to account. A combined analytical and

experimental study has been conducted by Wang and Qiao (Wang and Qiao 2007) to develop efficient and effective damage detection techniques for beam-type structures. The uniform load surface (ULS) has been employed in this study due to its less sensitivity to ambient noise. In combination with the ULS, two new damage detection algorithms, i.e., the generalized fractal dimension (GFD) and simplified gapped-smoothing (SGS) methods, has been proposed. Both methods are then applied to the ULS of cracked and delaminated beams obtained analytically, from which the damage location and size are determined successfully. Based on the experimentally measured curvature mode shapes, both the GFD and SGS methods are further applied to detect three different types of damage in carbon/epoxy composite beams. Damage detection in vibrating beams or beam systems has been done by Fabrizio and Danilo (Fabrizio and Danilo 2000) by discussing the amount of frequencies necessary to locate and quantify the damage uniquely. Two different procedures of damage identification are used, which mainly take advantage of the peculiar characteristics of the problem. Cases with pseudo experimental and experimental frequencies are solved.

The crack can be simulated by an equivalent spring, connecting the two segments of the beam, as stated by Narkis (Narkis 1994). Analysis of this approximate model results in algebraic equations which relate the natural frequencies of beam and crack characteristics. These expressions are then applied to studying the inverse problem—identification of crack location from frequency measurements. It is found that the only information required for accurate crack identification is the variation of the first two natural frequencies due to the crack, with no other information needed concerning the beam geometry or material and the crack depth or shape. The proposed method is confirmed by comparing it with results of numerical finite element calculations. The local effect of softening at the crack location can be simulated by an equivalent spring connecting the two segments of the beam as investigated by Wang et al (Wang *et al.* 2006). The model uses the transfer matrix method in conjunction with the Bernoulli-Euler theories of beam vibration, modal analysis and fracture mechanics principle to derive characteristic equation, which relates the natural frequencies. The proposed approach is verified by simulation results. Least square identification method, Kalman filtering method and adaptive filtering method have been adopted by Nian *et al.* (Nian *et al.* 1989) to diagnose structural fault.

The equation of motion and corresponding boundary conditions has been developed by Behzad et al. (Behzad et al. 2005) for forced bending vibration analysis of a beam with an open edge crack. A uniform Euler-Bernoulli beam and the Hamilton principle have been used in this research. The crack has been modeled as a continuous disturbance function in displacement filed which is obtained from fracture mechanics. They have stated that there is an agreement between the theoretical results and those obtained by the finite element method. The natural frequencies have been obtained by Loya et al. (Loya et al. 2006) for bending vibrations of Timoshenko cracked beams with simple boundary conditions. The beam is modeled as two segments connected by two mass less springs (one extensional and another one rotational). This model promotes discontinuities in both vertical displacement and rotation due to bending, which are proportional to shear force and bending moment transmitted by the cracked section, respectively. Their results show that their method provides simple expressions for the natural frequencies of cracked beams and it gives good results for shallow cracks. An extensive study has been made on diagnosis of fracture damage in structure by Akgun et al. (Akgun et al. 1983). The concept of 'fracture hinge' has been developed analytically and the same has been applied to a cracked section for detecting

fracture damage in simple structures. It has been verified experimentally that the structural effect of a cracked section can be represented by an equivalent spring loaded hinge. A fuzzy finite element method has been used by Chen and Rao (Chen and Rao 1997) for vibration analysis of imprecisely defined systems by using a search-based algorithm. The approach enhances the computational efficiency in fuzzy operations for identifying the system dynamic responses. A fuzzy arithmetical approach has been used by Hanss and Willner (Hanss and Willner 2000) for the solution of finite element problems involving uncertain parameters. Fuzzy finite element method for static analysis of engineering systems has been done by Rao and Sawayar (Rao and Sawayar 1995) using an optimization-based scheme taking fuzzy parameters, geometry and applied loads into consideration. The mobile robot navigation control system has been designed by Parhi (Parhi 2005) using fuzzy logic. Fuzzy rules embedded in the controller of a mobile robot enable it to avoid obstacles in a cluttered environment that includes other mobile robots. A fuzzy finite element approach has been used by Akpan et al. (Akpan *et al.* 2001) for modeling smart structures with vague or imprecise uncertainties.

The objective of the present study is to develop a systematic approach for damage detection of cracked beam structures using fuzzy logic technique. First, theoretical expressions have been developed to find out the effect of crack depth and crack location on natural frequencies and mode shapes of the beam structure that helps in generating fuzzy rules. These fuzzy rules are used in the fuzzy controller for prediction of damage location and intensity taking relative natural frequencies and relative mode shapes as input. Gaussian member ship functions are used in the fuzzy controller. The fuzzy controller results are also compared with the experimental and numerical results to verify the viability of fuzzy controller developed. The comparison shows a very good agreement.

2 THEORETICAL ANALYSIS

2.1 Local flexibility of a Cracked Beam Under Bending and Axial Loading

The presence of a transverse surface crack of depth 'a_1' on beam of width 'B' and height 'W' introduces a local flexibility, which can be defined in matrix form, the dimension of which depends on the degrees of freedom. Here a 2x2 matrix is considered. A cantilever beam is subjected to axial force (P_1) and bending moment (P_2), shown in figure 1a, which gives coupling with the longitudinal and transverse motion.

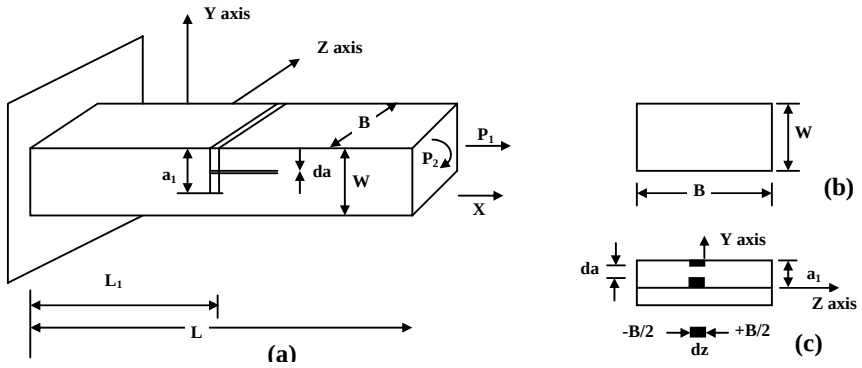

Figure 1: Geometry of beam, (a) Cantilever beam, (b) Cross-sectional view of the beam. (c) Segments taken during integration at the crack section

The strain energy release rate at the fractured section can be written as (Tada *et al*.1973);

$$J=\frac{1}{E'}(K_{I1}+K_{I2})^2, \text{ Where } \frac{1}{E'}=\frac{1-v^2}{E'} \text{ (for plane strain condition);}$$
$$= \frac{1}{E}\text{(for plane stress condition)}$$

$K_{I1,}$ K_{I2} are the stress intensity factors of mode I (opening of the crack) for load P_1 and P_2 respectively. The values of stress intensity factors from earlier studies (Tada *et al.* 1973) are;

$$K_{I1}=\frac{P_1}{BW}\sqrt{\pi a}\,(F_1(\frac{a}{W})), K_{I2}=\frac{6P_2}{BW^2}\sqrt{\pi a}\,(F_2(\frac{a}{W}))$$

Where expressions for F_1 and F_2 are as follows

$$F_1(\frac{a}{W}), =(\frac{2W}{\pi a}\tan(\frac{\pi a}{2W}))^{0.5}\left\{\frac{0.752+2.02(a/W)+0.37(1-\sin(\pi a/2W))^3}{\cos(\pi a/2W)}\right\}$$

$$F_2(\frac{a}{W}), =(\frac{2W}{\pi a}\tan(\frac{\pi a}{2W}))^{0.5}\left\{\frac{0.923+0.199(1-\sin(\pi a/2W))^4}{\cos(\pi a/2W)}\right\}$$

Let U_t be the strain energy due to the crack. Then from Castigliano's theorem, the additional displacement along the force P_i is:

$$u_i=\frac{\partial U_t}{\partial P_i} \tag{1}$$

The strain energy will have the form, $U_t=\int_0^{a_1}\frac{\partial U_t}{\partial a}da=\int_0^{a_1}J\,da$ (2)

Where J= $\frac{\partial U_t}{\partial a}$ the strain energy density function.

From equations (1) and (2), thus we have

$$u_i=\frac{\partial}{\partial P_i}\left[\int_0^{a_1}J(a)\,da\right] \tag{3}$$

The flexibility influence co-efficient C_{ij} will be, by definition

$$C_{ij}=\frac{\partial u_i}{\partial P_j}=\frac{\partial^2}{\partial P_i\partial P_j}\int_0^{a_1}J(a)\,da \tag{4}$$

To find out the final flexibility matrix we have to integrate over the breadth 'B'

$$C_{ij} = \frac{\partial u_i}{\partial P_j} = \frac{\partial^2}{\partial P_i \partial P_j} \int_{-B/2}^{+B/2} \int_0^{a_1} J(a)\, da\, dz \tag{5}$$

Putting the value strain energy release rate from above, equation (5) modifies as

$$C_{ij} = \frac{B}{E'} \frac{\partial^2}{\partial P_i \partial P_j} \int_0^{a_1} (K_{1I} + K_{12})^2\, da \tag{6}$$

Putting $\xi = (a/w), d\xi = \frac{da}{W}$,

We get $da = Wd\xi$ and when $a = 0, \xi = 0$; $a = a_1, \xi = a_1/W = \xi_1$

From the above condition equation (6) converts to,

$$C_{ij} = \frac{BW}{E'} \frac{\partial^2}{\partial P_i \partial P_j} \int_0^{\xi_1} (K_{1I} + K_{12})^2\, d\xi \tag{7}$$

From the equation (7), calculating C_{11}, C_{12} (=C_{21}) and C_{22} we get

$$C_{11} = \frac{BW}{E'} \int_0^{\xi_1} \frac{\pi a}{B^2 W^2} 2(F_1(\xi))^2\, d\xi$$

$$= \frac{2\pi}{BE'} \int_0^{\xi_1} \xi (F_1(\xi))^2\, d\xi \tag{8}$$

$$C_{12} = C_{21} = \frac{12\pi}{E'BW} \int_0^{\xi_1} \xi F_1(\xi) F_2(\xi)\, d\xi \tag{9}$$

$$C_{22} = \frac{72\pi}{E'BW^2} \int_0^{\xi_1} \xi F_2(\xi) F_2(\xi)\, d\xi \tag{10}$$

Converting the influence co-efficient into dimensionless form

$$\overline{C_{11}} = C_{11} \frac{BE'}{2\pi} \qquad \overline{C_{12}} = C_{12} \frac{E'BW}{12\pi} = \overline{C_{21}}\ ;\ \overline{C_{22}} = C_{22} \frac{E'BW^2}{72\pi}$$

The local stiffness matrix can be obtained by taking the inversion of compliance matrix. i.e.

$$K = \begin{bmatrix} K_{11} & K_{12} \\ K_{21} & K_{22} \end{bmatrix} = \begin{bmatrix} C_{11} & C_{12} \\ C_{21} & C_{22} \end{bmatrix}^{-1}$$

Figure 2 shows the variation of dimensionless compliances to that of relative crack depth.

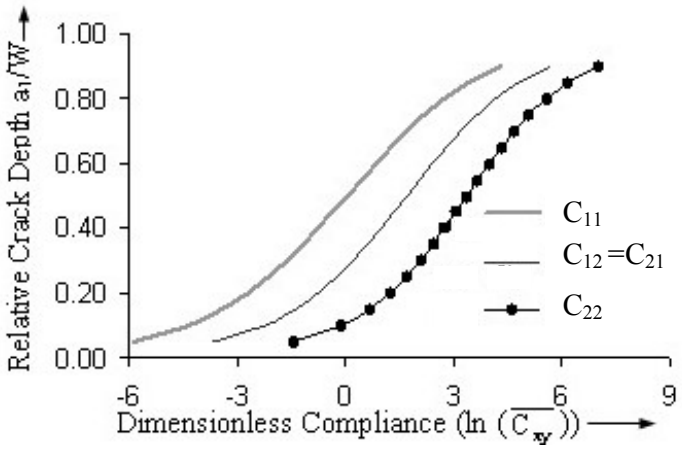

Figure 2: Relative crack depth (a_1/w) vs. dimensionless compliance (ln ($\overline{C_{xy}}$))

2.2 Analysis of Vibration Characteristics of the Cracked Beam

2.2.1 Free Vibration

A cantilever beam of length 'L' width 'B' and depth 'W', with a crack of depth 'a_1' at a distance 'L_1' from the fixed end is considered shown in figure 1. Taking $u_1(x, t)$ and $u_2(x, t)$ as the amplitudes of longitudinal vibration for the sections before and after the crack and $y_1(x, t)$, $y_2(x, t)$ are the amplitudes of bending vibration for the same sections shown in figure 3.

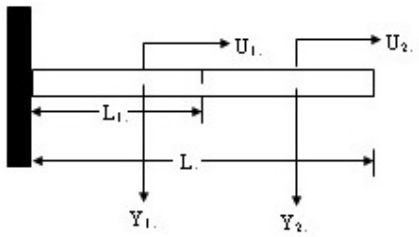

Figure 3: Beam model

The normal function for the system can be defined as

$$\bar{u}_1(\bar{x}) = A_1 \cos(\bar{K}_u \bar{x}) + A_2 \sin(\bar{K}_u \bar{x}) \quad (11a)$$

$$\bar{u}_2(\bar{x}) = A_3 \cos(\bar{K}_u \bar{x}) + A_4 \sin(\bar{K}_u \bar{x}) \quad (11b)$$

$$\bar{y}_1(\bar{x}) = A_5 \cosh(\bar{K}_y \bar{x}) + A_6 \sinh(\bar{K}_y \bar{x}) + A_7 \cos(\bar{K}_y \bar{x}) + A_8 \sin(\bar{K}_y \bar{x}) \quad (11c)$$

$$\bar{y}_2(\bar{x}) = A_9 \cosh(\bar{K}_y \bar{x}) + A_{10} \sinh(\bar{K}_y \bar{x}) + A_{11} \cos(\bar{K}_y \bar{x}) + A_{12} \sin(\bar{K}_y \bar{x}) \quad (11d)$$

Where $\bar{x} = \frac{x}{L}, \bar{u} = \frac{u}{L}, \bar{y} = \frac{y}{L}, \beta = \frac{L_1}{L}$

$$\bar{K}_u = \frac{\omega L}{C_u}, C_u = \left(\frac{E}{\rho}\right)^{1/2}, \bar{K}_y = \left(\frac{\omega L^2}{C_y}\right)^{1/2}, C_y = \left(\frac{EI}{\mu}\right)^{1/2}, \mu = A\rho$$

A_i, (i=1, 12) Constants are to be determined, from boundary conditions. The boundary conditions of the cantilever beam in consideration are:

$$\bar{u}_1(0) = 0; \quad \bar{y}_1(0) = 0; \quad \bar{y}_1'(0) = 0; \quad \bar{u}_2'(1) = 0; \quad \bar{y}''_2(1) = 0; \quad \bar{y}_2'''(1) = 0$$

At the cracked section:

$$\bar{u}_1(\beta) = \bar{u}_2(\beta); \quad \bar{y}_1(\beta) = \bar{y}_2(\beta); \quad \bar{y}_1''(\beta) = \bar{y}_2''(\beta); \quad \bar{y}_1'''(\beta) = \bar{y}_2'''(\beta)$$

Also at the cracked section, we have:

$$AE\frac{du_1(L_1)}{dx} = K_{11}(u_2(L_1) - u_1(L_1)) + K_{12}\left(\frac{dy_2(L_1)}{dx} - \frac{dy_1(L_1)}{dx}\right)$$

Multiplying both sides of the above equation by $\frac{AE}{LK_{11}K_{12}}$ we get;

$$M_1 M_2 \bar{u}'(\beta) = M_2(\bar{u}_2(\beta) - \bar{u}_1(\beta)) + M_1(\bar{y}_2'(\beta) - \bar{y}_1'(\beta))$$

Similarly, $EI\frac{d^2 y_1(L_1)}{dx^2} = K_{21}(u_2(L_1) - u_1(L_1)) + K_{22}\left(\frac{dy_2(L_1)}{dx} - \frac{dy_1(L_1)}{dx}\right)$

Multiplying both sides of the above equation by $\frac{EI}{L^2 K_{22} K_{21}}$ we get,

$$M_3 M_4 \bar{y}_1''(\beta) = M_3(\bar{u}_2(\beta) - \bar{u}_1(\beta)) + M_4(\bar{y}_2'(\beta) - \bar{y}_1'(\beta))$$

Where, $M_1 = \frac{AE}{LK_{11}}, M_2 = \frac{AE}{K_{12}}, M_3 = \frac{EI}{LK_{22}}, M_4 = \frac{EI}{L^2 K_{21}}$

The normal functions, equation (11) along with the boundary conditions as mentioned above, yield the characteristic equation of the system as:

$$|Q| = 0 \quad (12)$$

This determinant is a function of natural circular frequency (ω), the relative location of the crack (β) and the local stiffness matrix (K) which in turn is a function of the relative crack depth (a_1/W).

2.2.2 Forced Vibration

If the cantilever beam with transverse crack is excited at its free end by a harmonic excitation ($Y=Y_0\sin(\omega t)$), the non-dimensional amplitude at the free end may be expressed as $\bar{y}_2(1)=\frac{y_0}{L}=\bar{y}_0$. Therefore the boundary conditions for the beam remain same as before except the boundary condition $\bar{y}_2''(1)=0$ which modified as $\bar{y}_2(1)=\bar{y}_0$

The constants A_i, i=1, to 12 are then computed from the algebraic condition

$$Q_1 D=B_1 \tag{13}$$

Q_1 is the (12 x 12) matrix obtained from boundary conditions as mentioned above,

D is a column matrix obtained from the constants,

B_1 is a column matrix, transpose of which is given by, $B_1^T=[0\,0\,0\,\bar{y}_0\,0\,0\,0\,0\,0\,0\,0\,0]$

3 ANALYSIS OF THE FUZZY CONTROLLER

The fuzzy controller developed has got six input parameters and two output parameters.

The linguistic term used for the inputs are as follows;

Relative first natural frequency = “fnf”; Relative second natural frequency = “snf”;

Relative third natural frequency = “tnf”; Relative first mode shape difference = “fmd”;

Relative second mode shape difference = “smd”;

Relative third mode shape difference = “tmd”.

The linguistic term used for the outputs are as follows;

Relative crack location = “rcl” and Relative crack depth = “rcd”

The Fuzzy controller used in the present text is shown in Figure 4a. The Gaussian membership functions are shown pictorially in Figure 4b. The linguistic terms for the Gaussian membership functions, used in the fuzzy controller, are described in the Table 1.

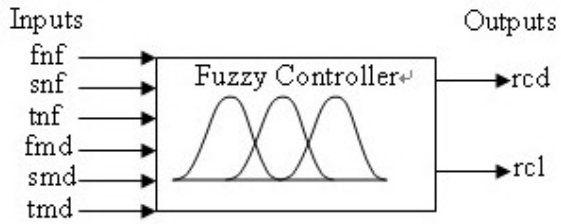

Figure 4a: Fuzzy controller

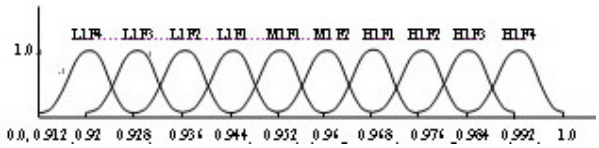

Figure 4b1: Membership functions for relative natural frequency for first mode of vibration

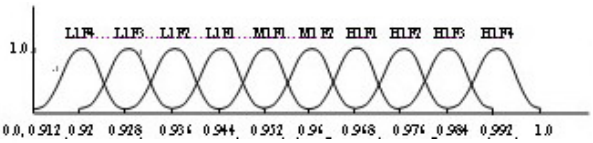

Figure 4b2: Membership functions for relative natural frequency for second mode of vibration

Figure 4b3: Membership functions for relative natural frequency for third mode of vibration

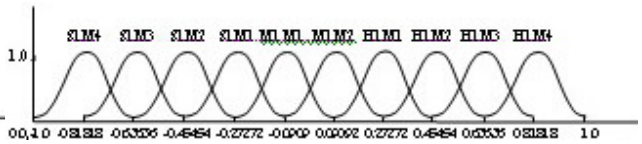

Figure 4b4: Membership functions for relative mode shape difference for first mode of vibration

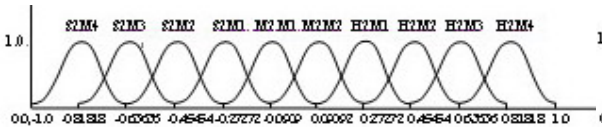

Figure 4b5: Membership functions for relative mode shape difference for second mode of vibration

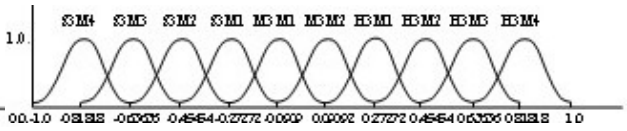

Figure 4b6: Membership functions for relative mode shape difference for third mode of vibration

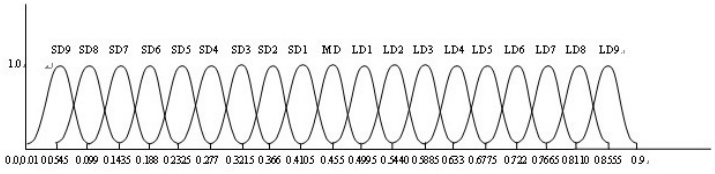

Figure 4b7: Membership functions for relative crack depth

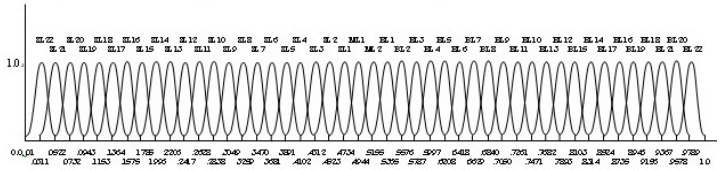

Figure 4b8: Membership functions for relative crack location

Table 1: Description of fuzzy Linguistic terms

Membership functions Name	Linguistic Terms	Description and range of the Linguistic terms
L1F1,L1F2,L1F3,L1F4	fnf $_{1 \text{ to } 4}$	Low ranges of relative natural frequency for first mode of vibration in descending order respectively
M1F1,M1F2	fnf $_{5,6}$	Medium ranges of relative natural frequency for first mode of vibration in ascending order respectively
H1F1,H1F2,H1F3,H1F4	fnf $_{7 \text{ to } 10}$	Higher ranges of relative natural frequency for first mode of vibration in ascending order respectively
L2F1,L2F2,L2F3,L2F4	snf $_{1 \text{ to } 4}$	Low ranges of relative natural frequency for second mode of vibration in descending order respectively
M2F1,M2F2	snf $_{5,6}$	Medium ranges of relative natural frequency for second mode of vibration in ascending order respectively
H2F1,H2F2,H2F3,H2F4	snf $_{7 \text{ to } 10}$	Higher ranges of relative natural frequencies for second mode of vibration in ascending order respectively
L3F1,L3F2,L3F3,L3F4	tnf $_{1 \text{ to } 4}$	Low ranges of relative natural frequencies for third mode of vibration in descending order respectively
M3F1,M3F2	tnf $_{5,6}$	Medium ranges of relative natural frequencies for third mode of vibration in ascending order respectively
H3F1,H3F2,H3F3,H3F4	tnf $_{7 \text{ to } 10}$	Higher ranges of relative natural frequencies for third mode of vibration in ascending order respectively
S1M1,S1M2,S1M3,S1M4	fmd $_{1 \text{ to } 4}$	Small ranges of first relative mode shape difference in descending order respectively
M1M1,M1M2	fmd $_{5,6}$	medium ranges of first relative mode shape difference in ascending order respectively
H1M1,H1M2,H1M3,H1M4	fmd $_{7 \text{ to } 10}$	Higher ranges of first relative mode shape difference in ascending order respectively
S2M1,S2M2,S2M3,S2M4	smd $_{1 \text{ to } 4}$	Small ranges of second relative mode shape difference in descending order respectively
M2M1,M2M2	smd $_{5,6}$	medium ranges of second relative mode shape difference in ascending order respectively
H2M1,H2M2,H2M3,H2M4	smd $_{7 \text{ to}10}$	Higher ranges of second relative mode shape difference in ascending order respectively
S3M1,S3M2,S3M3,S3M4	tmd $_{1 \text{ to } 4}$	Small ranges of third relative mode shape difference in descending order respectively
M3M1,M3M2	tmd $_{5,6}$	medium ranges of third relative mode shape difference in ascending order respectively
H3M1,H3M2,H3M3,H3M4	tmd $_{7 \text{ to } 10}$	Higher ranges of third relative mode shape difference in ascending order respectively
SL1,SL2……SL22	rcl $_{1 \text{ to } 22}$	Small ranges of relative crack location in descending order respectively
ML1,ML2	rcl $_{23,24}$	Medium ranges of relative crack location in ascending order respectively
BL1,BL2…….BL22	rcl $_{25 \text{ to } 46}$	Bigger ranges of relative crack location in ascending order respectively
SD1,SD2……SD9	rcd $_{1 \text{ to } 9}$	Small ranges of relative crack depth in descending order respectively
MD	rcd $_{10}$	Medium relative crack depth
LD1,LD2……LD9	rcd $_{11 \text{ to } 19}$	Larger ranges of relative crack depth in ascending order respectively

3.1 Fuzzy Mechanism for Crack Detection

Based on the above fuzzy subsets, the fuzzy control rules are defined in a general form as follows:

If (fnf is fif_i and snf is snf_j and tnf is tnf_k and fmd_l and smd is smd_m and tmd is tmd_n) then rcl is rcl_{ijklmn} and rcd is rcd_{ijklmn} (14)

where i=1 to 10, j=1 to 10, k = 1 to 10, l= 1 to 10, m= 1 to 10, n= 1 to 10

Because "fnf", "snf", "tnf", "fmd", "smd", "tmd" have ten membership functions each.

From expression (14), two set of rules can be written

$$\left.\begin{array}{l}\text{If (fnf is } fnf_i \text{ and snf is } snf_j \text{ and tnf is } tnf_k \text{ and fmd is } fmd_l \text{ and smd is } smd_m \text{ and tmd is } tmd_n) \\ \text{then rcd is } rcd_{ijklmn} \\ \\ \text{If (fnf is } fnf_i \text{ and snf is } snf_j \text{ and tnf is } tnf_k \text{ and fmd is } fmd_l \text{ and smd is } smd_m \text{ and tmd is } tmd_n) \\ \text{then rcl is } rcd_{ijklmn}\end{array}\right\} \quad (15)$$

According to the usual fuzzy logic control method Parhi (Parhi 2005), a factor W_{ijklmn} is defined for the rules as follows:

$$W_{ijklmn} = \mu_{fnf_i}(freq_i) \wedge \mu_{snf_j}(freq_j) \wedge \mu_{tnf_k}(freq_k) \wedge \mu_{fmd_l}(moddif_l) \wedge \mu_{smd_m}(moddif_m) \wedge \mu_{tmd_n}(moddif_n)$$

Where $freq_i$, $freq_j$ and $freq_k$ are the first , second and third relative natural frequencies of the cantilever beam with crack respectively ; $moddif_l$, $moddif_m$ and $moddif_n$ are the first, second and third relative mode shape differences of the cantilever beam with crack respectively. By applying the composition rule of inference Parhi (Parhi 2005), the membership values of the relative crack location and relative crack depth, $(location)_{rcl}$ and $(depth)_{rcd}$ can be computed as;

$$\left.\begin{array}{ll}\mu_{rcl_{ijklmn}}(location) = W_{ijklmn} \wedge \mu_{rcl_{ijklmn}}(location) & \forall_{length} \in rcl \\ \mu_{rcd_{ijklmn}}(depth) = W_{ijklmn} \wedge \mu_{rcd_{ijklmn}}(depth) & \forall_{depth} \in rcd\end{array}\right\} \quad (16)$$

The overall conclusion by combining the outputs of all the fuzzy rules can be written as follows:

$$\left.\begin{array}{l}\mu_{rcl}(location) = \mu_{rcl_{111111}}(location) \vee .... \vee \mu_{rcl_{ijklmn}}(location) \vee ..... \vee \mu_{rcl_{10\ 10\ 10\ 10\ 10\ 10}}(location) \\ \mu_{rcd}(depth) = \mu_{rcd_{111111}}(depth) \vee ..... \vee \mu_{rcd_{ijklmn}}(depth) \vee ..... \vee \mu_{rcd_{10\ 10\ 10\ 10\ 10\ 10}}(depth)\end{array}\right\} \quad (17)$$

The crisp values of relative crack location and relative crack depth are computed using the centre of gravity method Parhi (Parhi 2005) as:

$$\left.\begin{aligned} \text{relative crack location} = \text{rcl} &= \frac{\int (\text{location} \cdot \mu_{\text{rcl}}(\text{location}) \cdot \text{d(location)}}{\int \mu_{\text{rcl}}(\text{location}) \cdot \text{d(location)}} \\ \text{relative crack depth} = \text{rcd} &= \frac{\int (\text{depth}) \cdot \mu_{\text{rcd}}(\text{depth}) \cdot \text{d(depth)}}{\int \mu_{\text{rcd}}(\text{depth}) \cdot \text{d(depth)}} \end{aligned}\right\} \quad (18)$$

3.2 Fuzzy Controller for Finding Out Crack Depth and Crack Location

The inputs to the fuzzy controller are relative first natural frequency; relative second natural frequency; relative third natural frequency; relative first mode shape difference; relative second mode shape difference and relative third mode shape difference. The outputs from the fuzzy controller are relative crack depth and relative crack location. Twenty numbers of the fuzzy rules out of several hundred fuzzy rules are being listed in table 2. Figure 5 shows the fuzzy controller results when the rule-7 and rule-19 are activated from table 2.

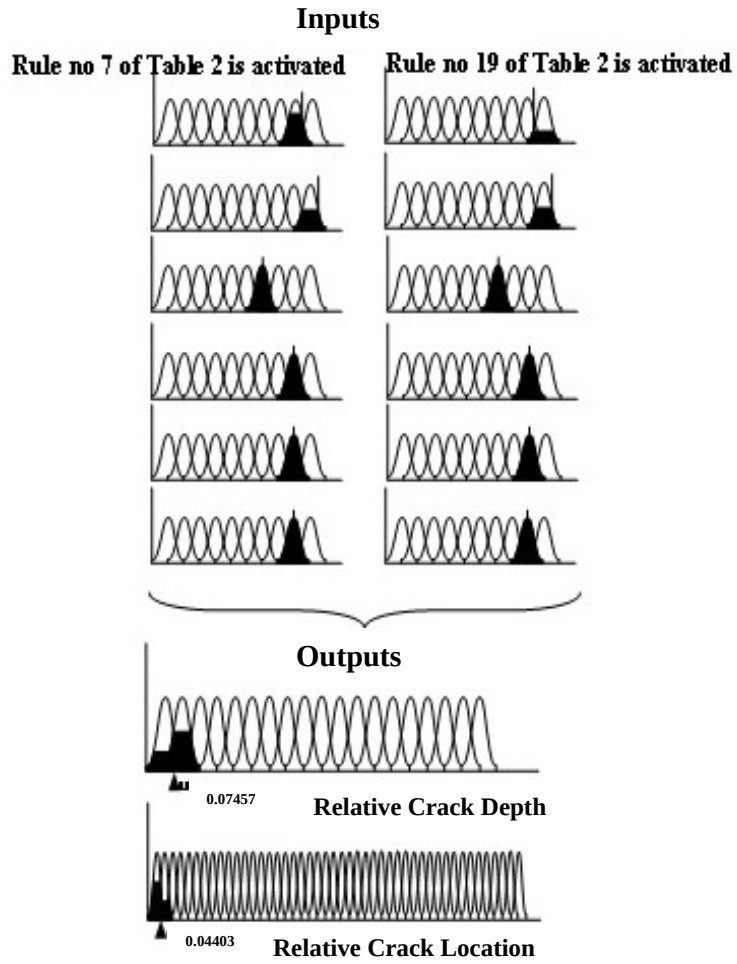

Figure 5: Resultant values of relative crack depth and relative crack location when Rules 7 and 19 of table 2 are activated.

Table 2: Examples of twenty fuzzy rules used in fuzzy controller.

Sl.No.	Examples of some rules used in the fuzzy controller
1	If fnf is H1F2,snf is M2F2,tnf is M3F2,fmd is H1M3,smd is H2M3,tmd is H3M9, then rcd is SD1,and rcl is SL20
2	If fnf is H1F3,snf is H2F3,tnf is H3F1,fmd is H1M3,smd is H2M3,tmd is H3M3, then rcd is SD8,and rcl is SL22
3	If fnf is H1F1,snf is M2F1,tnf is L3F2,fmd is H1M4,smd is H2M4,tmd is H3M4, then rcd is MD,and rcl is SL22
4	If fnf is M1F1,snf is L2F2,tnf is L3F2,fmd is H1M4,smd is H2M4,tmd is H3M4, then rcd is LD5,and rcl is SL22
5	If fnf is H1F1,snf is M2F1,tnf is L3F1,fmd is H1M3,smd is H2M3,tmd is H3M3, then rcd is LD1,and rcl is SL21
6	If fnf is M1F1,snf is L2F1,tnf is L3F2,fmd is H1M4,smd is H2M3,tmd is H3M4, then rcd is LD6,and rcl is SL21
7	If fnf is H1F3,snf is H2F4,tnf is H3F1,fmd is H1M3,smd is H2M3,tmd is H3M3, then rcd is SD8,and rcl is SL22
8	If fnf is H1F3,snf is H2F4,tnf is H3F2,fmd is H1M2,smd is H2M1,tmd is H3M2, then rcd is SD7,and rcl is SL19
9	If fnf is H1F1,snf is M2F2,tnf is H3F2,fmd is H1M2,smd is H2M2,tmd is H3M2, then rcd is LD2,and rcl is SL18
10	If fnf is H1F3,snf is H2F4,tnf is H3F3,fmd is S1M1,smd is S2M1,tmd is S3M1, then rcd is SD3,and rcl is SL17
11	If fnf is H1F1,snf is H2F3,tnf is H3F2,fmd is H1M2,smd is H2M1,tmd is H3M1, then rcd is LD2,and rcl is SL16
12	If fnf is H1F2,snf is H2F4,tnf is H3F2,fmd is H1M2,smd is M2M2,tmd is H3M2, then rcd is LD1,and rcl is SL15
13	If fnf is H1F2,snf is H2F4,tnf is H3F1,fmd is H1M2,smd is M2M2,tmd is H3M2, then rcd is MD,and rcl is SL14
14	If fnf is M1F2,snf is M2F1,tnf is L3F3,fmd is H1M2,smd is H2M2,tmd is H3M3, then rcd is LD9,and rcl is SL7
15	If fnf is H1F1,snf is H2F4,tnf is M3F1,fmd is H1M2,smd is M2M2,tmd is H3M3, then rcd is LD4,and rcl is SL13
16	If fnf is H1F3,snf is H2F4,tnf is M3F1,fmd is H1M2,smd is H2M1,tmd is H3M3, then rcd is SD2,and rcl is SL10
17	If fnf is M1F1,snf is M2F2,tnf is L3F3,fmd is H1M2,smd is H2M2,tmd is H3M3, then rcd is LD9,and rcl is SL9
18	If fnf is H1F2,snf is H2F4,tnf is L3F1,fmd is H1M2,smd is M2M1,tmd is H3M3, then rcd is LD3,and rcl is SL12
19	If fnf is H1F4,snf is H2F4,tnf is H3F1,fmd is H1M3,smd is H2M3,tmd is H3M3, then rcd is SD9,and rcl is SL21
20	If fnf is H1F4,snf is H2F3,tnf is M3F2,fmd is M1M1,smd is H2M2,tmd is H3M3, then rcd is SD4,and rcl is BL7

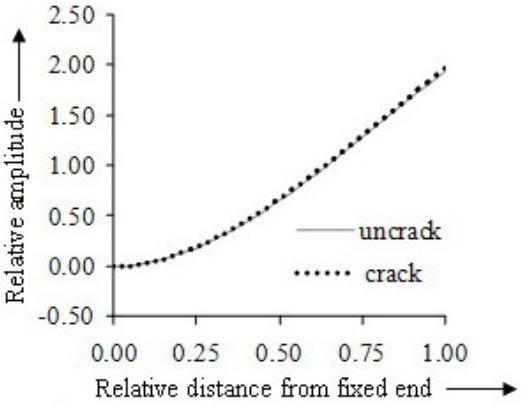

Figure 6a: Relative amplitude vs. relative distance from the fixed end (1st mode of vibration), $a_1/W=0.3$, $L_1/L=0.0256$

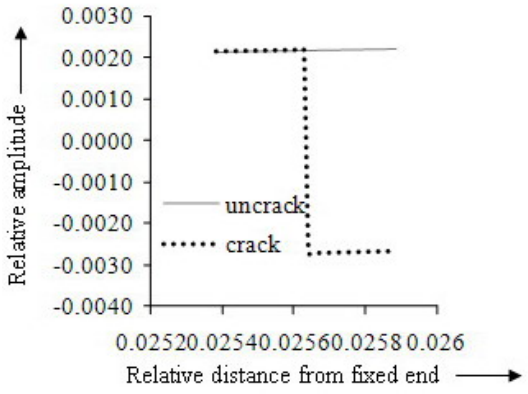

Figure 6a1: Magnified view of figure: 6a at the vicinity of the crack location

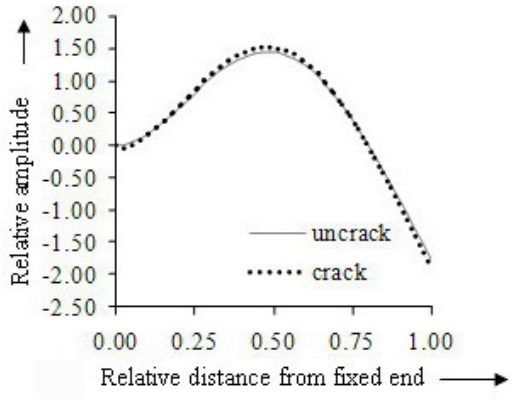

Figure 6b: Relative amplitude vs. relative distance from the fixed end (2nd mode of vibration), $a_1/W=0.3$, $L_1/L=0.0256$

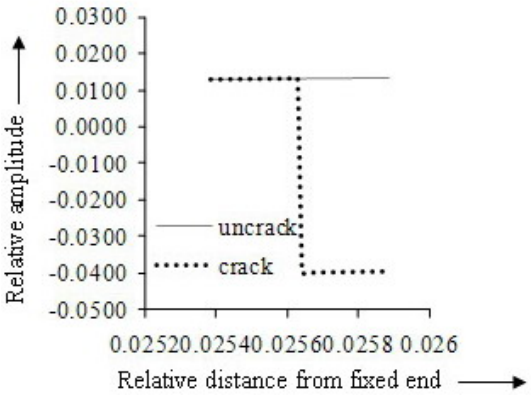

Figure 6b1: Magnified view of Figure: 6b at the vicinity of the crack location.

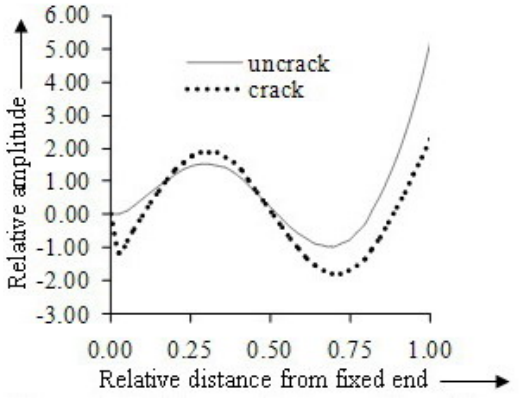

Figure: 6c Relative amplitude vs. relative distance from the fixed end (3rd mode of vibration), $a_1/W=0.3$, $L_1/L=0.0256$

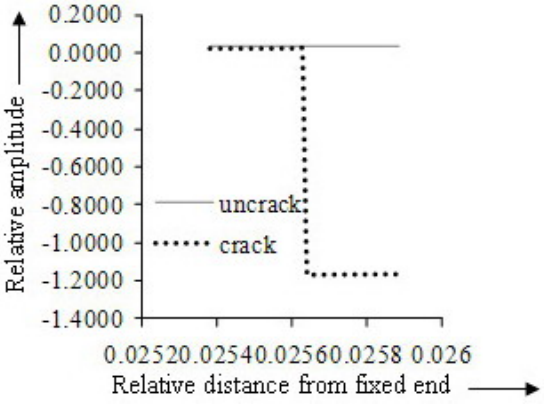

Figure 6c1: Magnified view of Figure: 6c1 at the vicinity of the crack location.

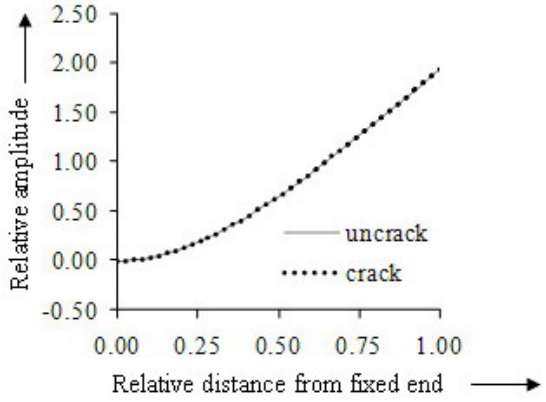

Figure 7a: Relative amplitude vs. relative distance from the fixed end (1st mode of vibration), $a_1/W=0.2$, $L_1/L=0.5128$

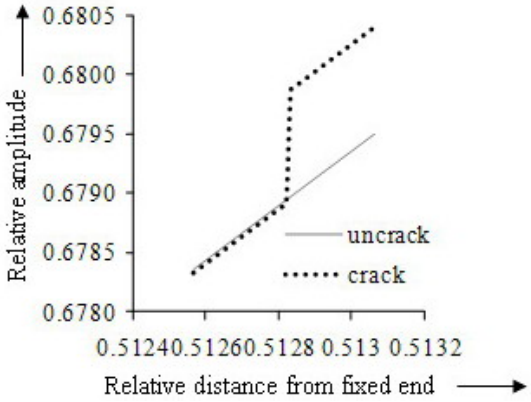

Figure 7a1: Magnified view of figure 7a at the vicinity of the crack location

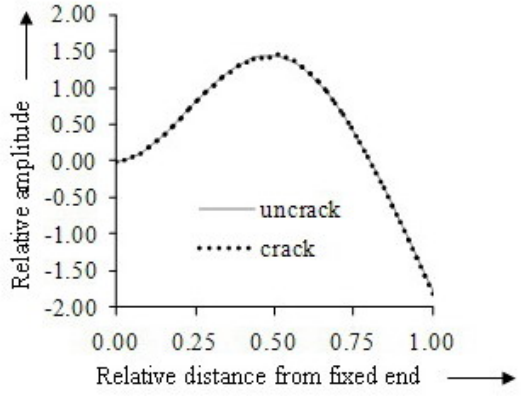

Figure 7b: Relative amplitude vs. relative distance from the fixed end (2nd mode of vibration), $a_1/W=0.2$, $L_1/L=0.5128$

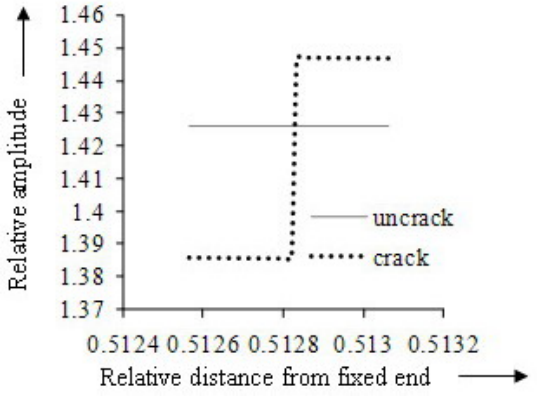

Figure: 7b1 Magnified view of figure 7b at the vicinity of the crack location

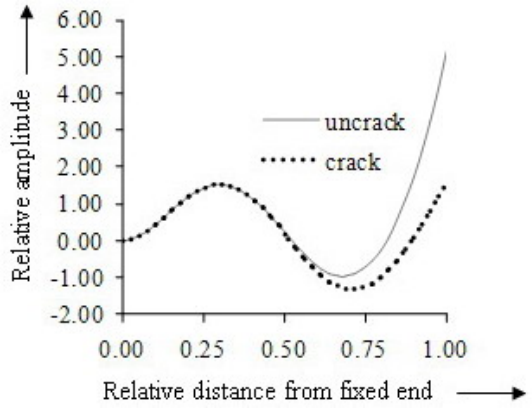

Figure: 7c Relative amplitude vs. relative distance from the fixed end (3rd mode of vibration), $a_1/W=0.2$, $L_1/L=0.5128$

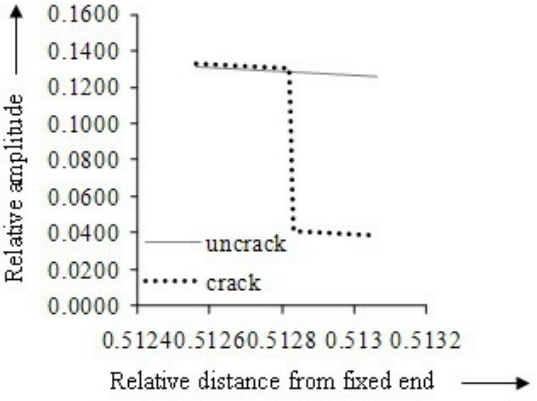

Figure: 7c1 Magnified view of figure 7c at the vicinity of the crack location

4 EXPERIMENTAL SET-UP

An experimental set-up used for performing the experiments is shown in schematic diagram Figure 8. A number of tests are conducted on Aluminium beam specimen (800 x 50 x 6mm) with a transverse crack for determining the natural frequencies and mode shapes for different crack depths. Experimental results of amplitude of transverse vibration at various locations along the length of the beam are recorded by positioning the vibration pick-up and tuning the vibration generator at the corresponding resonant frequencies. These results for first three modes are plotted in Figure 9. Corresponding numerical results are also presented in the same graph for comparison.

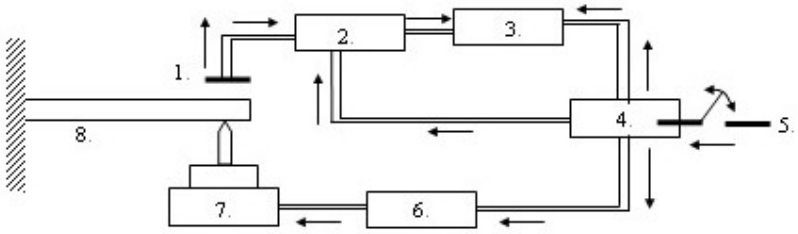

1. Vibration Pick-up
2. Amplifier
3. Vibration indicator
4. Distribution box
5. Power supply
6. Power amplifier
7. Vibration generator
8. Cantilever beam

Figure 8: Schematic block diagram of experimental set-up

Table 3: Comparison of results between fuzzy controller, numerical analysis and experimental setup

Relative first natural frequency "fnf"	Relative second natural frequency "snf"	Relative third natural frequency "tnf"	Relative first mode shape difference "fmd"	Relative second mode shape difference "smd"	Relative third mode shape difference "tmd"	Fuzzy Controller (relative crack depth "rcd" and location"rcl")		Numerical (relative crack depth "rcd" and location"rcl")		Experimental (relative crack depth "rcd" and location"rcl")	
						rcd	rcl	rcd	rcl	rcd	rcl
0.9848	0.9958	0.9975	0.2709	0.2372	0.3158	0.203	0.072	0.202	0.069	0.205	0.073
0.9673	0.9874	0.9943	0.3969	0.3247	0.3923	0.431	0.082	0.427	0.079	0.43	0.084
0.9623	0.9948	0.9983	0.1814	0.0279	0.0774	0.548	0.16	0.537	0.16	0.568	0.158
0.9756	0.9976	0.9972	0.1383	-0.0823	0.1898	0.389	0.188	0.394	0.187	0.391	0.188
0.9852	0.9984	0.9967	0.01	-0.8678	0.2572	0.227	0.237	0.231	0.237	0.23	0.24
0.9723	0.9961	0.9818	0.1947	0.0672	0.4105	0.552	0.284	0.556	0.283	0.545	0.287
0.9823	0.9872	0.9919	0.0726	0.2567	0.3994	0.449	0.405	0.451	0.404	0.447	0.406
0.981	0.9809	0.9931	0.0898	0.3154	0.392	0.495	0.424	0.497	0.424	0.495	0.424
0.986	0.9842	0.9988	-0.032	0.322	0.3965	0.425	0.502	0.426	0.502	0.425	0.504
0.9834	0.9685	0.9974	0.038	0.4558	0.3507	0.537	0.534	0.542	0.535	0.535	0.534

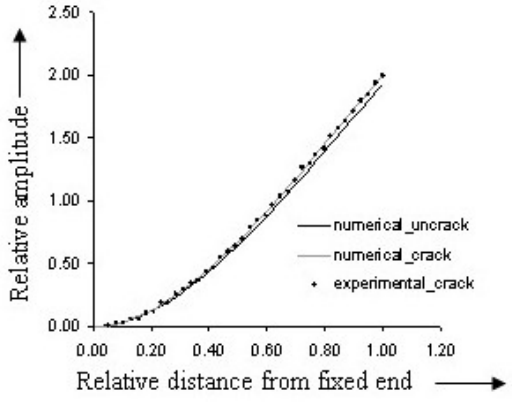

Figure 9a: Relative amplitude vs. relative distance from the fixed end (1st mode of vibration), $a_1/W=0.4$, $L_1/L=0.0256$

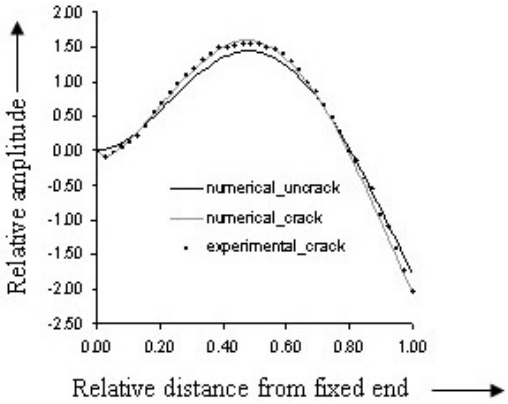

Figure 9b: Relative amplitude vs. relative distance from the fixed end (2nd mode of vibration), $a_1/W=0.4$, $L_1/L=0.0256$

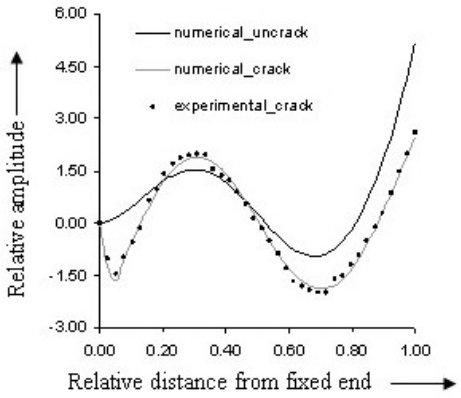

Figure 9c: Relative amplitude vs. relative distance from the fixed end (3rd mode of vibration), $a_1/W=0.4$, $L_1/L=0.0256$

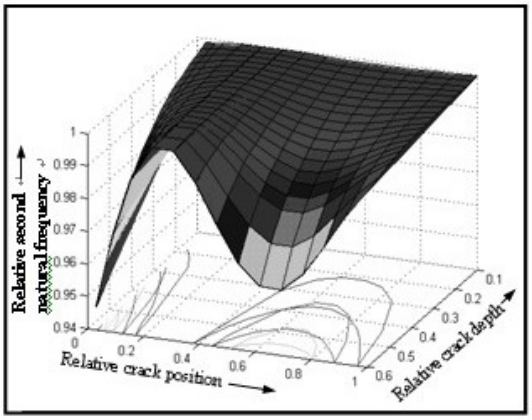

Figure 10: Three dimensional cum contour plot for relative natural frequency

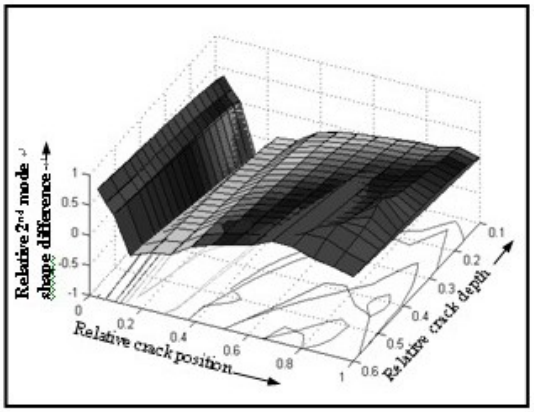

Figure 11: Three dimensional cum contour plot for relative mode shape difference

5 DISCUSSION

Discussions based on the outputs of fuzzy controller used and information supplemented by numerical and experimental analyses are mentioned below. It can be noticed from graph of figure 2 that the compliances (C_{11}, C_{12}, = C_{21}, C_{22}) increase with the increase in relative crack depth. The linguistic form of fuzzy rules established for fuzzy membership functions used in the present fuzzy controller are given in table 1. Some of the sample examples of actual rules made for the fuzzy controller of the present investigation are listed In table 2. The present fuzzy controller uses Gaussian membership functions that are depicted in figure 4. The outputs of the Gaussian- Fuzzy controller obtained by activating rule-7 and rule-19 from the table 2 are presented in figure 5. The relation between the relative beam length from the fixed end and relative amplitude, for three modes of vibrations, are shown in graphical form in figure 6 and figure 7 for different relative crack locations (0.0256, 0.5128) and relative crack depths (0.3, 0.2). It can be observed from these figures that there are significant variations in mode shapes at the vicinity of crack location due to the presence of crack. The mode shapes obtained from experimental and numerical analyses for cracked and uncracked beam are compared graphically in figure 9. The relation between relative natural frequencies, relative crack locations and relative crack depths are depicted graphically in figure 10 along with the respective contour graphs. The three dimensional graphs along with the respective contour graphs showing the variation of relative mode shapes with respect to relative crack locations and relative crack depths are represented in figure 11.Some of the predicted outputs of the developed fuzzy controller and corresponding numerical and experimental results are presented in table 3. It is observed that the results of all analyses are in well agreement.

6 CONCLUSION

The present investigation basing on the analytical and experimental results and discussions draws the following conclusions.

Significant changes in natural frequencies and mode shapes of the vibrating beam are observed at the vicinity of crack location.

The fuzzy controller is developed with Gaussian member ship functions.

The inputs parameters to the fuzzy controller are first three relative natural frequencies and first three mode shapes in dimensionless forms. The outputs from the fuzzy controller are relative crack location and relative crack depth.

By comparing the fuzzy results with the experimental results it is observed that the developed fuzzy controller can predict the relative crack location and relative crack depth in a very accurate manner.

The crack depth and crack location of a beam can be predicted by the developed fuzzy controller in nano seconds thereby saving a considerable amount of computational time.

Further research can be made in the future to generate hybrid fuzzy controller for more efficient results.

REFERENCES

Akgun M, Ju FD, and Pacz TL (1983). "Fracture diagnosis in beam frame structures using circuit analogy". *Rec. Adr. Engineering Mechanical and Impact in Ce Practice*, 2, pp.767-769.

Akpan UO, Koko TS, Orisamolu IR, and Gallant BK (2001). "Fuzzy finite-element analysis of smart structures". *Smart Materials and Structures*, 10, pp.273–284.

Behzad M, Meghdari A, and Ebrahimi A (2005). "A continuous model for forced vibration analysis of a cracked beam". *American Society of Mechanical Engineers, Dynamic Systems and Control Division (Publication)*, DSC 74 DSC (2 ART B), pp. 1849-1855.

Behzad M, Meghdari A, and Ebrahimi A (2005). "A new approach for vibration analysis of a cracked beam". *International Journal of Engineering, Transactions B: Applications*, 18 (4), pp.319-330.

Chen L and Rao SS (1997). "Fuzzy finite-element approach for the vibration analysis of imprecisely-defined systems". *Finite Elements n Analysis and Design*, 27, pp.69–83.

Fabrizio V and Danilo C (2000). "Damage detection in beam structures based on frequency measurements". *J. Engrg. Mech*, 126(7), pp. 761-768.

Hanss M and Willner K (2000). "A fuzzy arithmetical approach to the solution of finite element problems with uncertain parameters". *Mechanics Research Communications*, 27(3), pp. 257–272.

Karthikeyan MA, Tiwari RA, and Talukdar SB (2007). "Crack localization and sizing in a beam based on the free and forced response measurement". *Mechanical Systems and Signal Processing*, 21(3), pp. 1362-1385.

Loya JA, Rubio L, and Fernández-Sáez J (2006). "Natural frequencies for bending vibrations of timoshenko cracked beams". *Journal of Sound and Vibration*, 290 (3-5), pp. 640-653.

Narkis Y (1994). "Identification of Crack Location in Vibrating Simply Supported Beams". *Journal of sound and vibration*, 172(4), pp. 548-558.

Nian GS, Lin ZJ, Sheng JJ, and An, HC (1989). "A vibration diagnosis approach to structural fault". *A.S.M.E. Journal of Vibration and Acoustics, Stress and Reliability in Design* III, pp. 88-93.

Parhi DR (2005). "Navigation of mobile robot using a fuzzy logic controller". *Journal of Intelligent and Robotic Systems: Theory and Applications*, 42(3), pp. 253-273.

Rao SS and Sawyer JP (1995). "A fuzzy element approach for the analysis of imprecisely-defined system". *AIAA Journal*, 33(12), pp. 2364–2370.

Tada H, Paris PC, and Irwin GR (1973). "*The stress analysis of cracks hand book*". Del Research Corp. Hellertown, Pennsylvanian.

Wang J and Qiao P (2007). "Improved damage detection for beam-type structures using a uniform load surface". *Structural Health Monitoring*, **6**(2), pp. 99-110.

Wang ZH, Zhao YG, and Ma HW (2006). "Investigation on crack identification in the beam-type structures". *Chinese Journal of Computational Mechanics*, 23(3), pp.307-312.